Combined Experimental and Theoretical Investigation of Three-Dimensional, Nitrogen-Doped, Gallium Cluster Anions†

Haopeng Wang, Yeon Jae Ko, and Kit H. Bowen*

Departments of Chemistry and Materials Science, Johns Hopkins University, Baltimore, Maryland 21218

Alina P. Sergeeva, Boris B. Averkiev, and Alexander I. Boldyrev*

Department of Chemistry and Biochemistry, Utah State University, 0300 Old Main Hill, Logan, Utah 84322-0300

Received: February 15, 2010; Revised Manuscript Received: March 23, 2010

Anion photoelectron spectra of $Ga_xN_y^-$ cluster anions, in which $x = 4-12$, $y = 1$ and $x = 7-12$, $y = 2$, were measured. Ab initio studies were conducted on $Ga_xN_y^-$ cluster anions in which $x = 4-7$, $y = 1$ and $Ga_7N_2^-$, providing their structures and electronic properties. The photoelectron spectra were interpreted in terms of the computational results. This allowed for identification of the isomers present in the beam experiments for specific Ga_xN^- cluster anions ($x = 4-7$). The unexpected presence of $Ga_xN_2^-$ species is also reported.

I. Introduction

Gallium nitride (GaN) is an important wide-band-gap semiconductor.[1,2] Despite the potential importance of gallium nitride, there have been relatively few studies, either experimental or theoretical, on gallium nitride clusters.[3–22] The combination of anion photoelectron spectroscopy (PES) with global minimum structure searches is an effective tool for determining geometrical structures of negatively charged clusters. A previous anion photoelectron spectroscopic study was performed on Ga_2N^- by Sheehan et al.[5] They recorded PES spectra of Ga_2N^- at 416, 355, and 266 nm. The spectra showed transitions to the ground and the first excited electronic states of neutral Ga_2N ($X\ ^2\Sigma_u^+ \rightarrow X\ ^1\Sigma_g^+$; $A\ ^2\Pi_u \rightarrow X\ ^1\Sigma_g^+$), leading to an electron affinity value of 2.506 ± 0.008 eV for Ga_2N.

In the current work, we present our joint anion photoelectron spectroscopic and ab initio study of a series of $Ga_xN_y^-$ clusters, in which $x = 4-7$, $y = 1$, and the $Ga_7N_2^-$ cluster, which was studied theoretically, and when $x = 4-12$, $y = 1$ and $x = 7-12$, $y = 2$, was studied experimentally. On the experimental side, we measured anion photoelectron spectra at 355 and 266 nm, that is, 3.49 and 4.66 eV, respectively. On the computational side, we computed the geometric and electronic structures of the Ga_xN^- clusters and the $Ga_7N_2^-$ cluster and interpreted the photoelectron spectra.

II. Experimental Methods

Anion photoelectron spectroscopy is conducted by crossing a mass-selected beam of negative ions with a fixed-frequency photon beam and energy-analyzing the resultant photodetached electrons. It is governed by the energy-conserving relationship, $h\nu = EBE + EKE$, where $h\nu$ is the photon energy, EBE is the electron binding (transition) energy, and EKE is the electron kinetic energy. Briefly, our apparatus, which has been described previously,[23] consists of a laser vaporization source, a time-of-flight mass spectrometer for mass analysis and mass selection, Nd:YAG lasers for ablation and for photodetachment, and a magnetic bottle electron energy analyzer. In the present work, $Ga_xN_y^-$ and Ga_x^- cluster anions were produced by laser-ablating a disk of pressed gallium nitride powder with 532 nm photons.

III. Theoretical Methods

We performed initial computational searches for the global minima of Ga_xN^- ($x = 4-7$) and $Ga_7N_2^-$ using both our Gradient Embedded Genetic Algorithm (GEGA) program written by A. N. Alexandrova[24,25] and the Coalescence Kick (CK) method written by B. B. Averkiev.[26] We first used a hybrid density functional method known in the literature as B3LYP[27–29] with the small split-valence basis set (3-21G) for energy, gradient, and force calculations. We then reoptimized geometries and calculated frequencies for the lowest isomers of Ga_xN^- (identified by GEGA and CK) at the B3LYP and CCSD(T)[30–32] (for small-sized clusters only) methods with the polarized split-valence basis set (6-311+G*).[33–35] Total energies of the lowest isomers were also calculated using the CCSD(T) method with the extended 6-311+G(2df) basis set.

The vertical electron detachment energies (VDEs) were calculated using the restricted (unrestricted) coupled cluster method with single, double, and noniterative triple excitations (R(U)CCSD(T)/6-311+G(2df) method), the restricted (unrestricted) Outer Valence Green Function method (R(U)OVGF/6-311+G(2df)),[36–40] and the time-dependent density functional method[41,42] (TD-B3LYP/6-311+G(2df)) for closed-shell (open-shell) Ga_xN^- clusters and for the closed-shell $Ga_7N_2^-$ cluster. In the TD-B3LYP approach, the first VDE was calculated at the B3LYP level of theory as the lowest-energy transition from the singlet state of the anion into the lowest-energy doublet state of the neutral (in the case of Ga_xN^- and $Ga_7N_2^-$ clusters' being in the singlet state) and as the lowest-energy transition from the doublet state of the anion into the lowest-energy singlet and triplet states of the neutral (in the case of Ga_xN^- cluster's being in the doublet state). Then the vertical excitation energies of the neutral species (calculated at the TD-B3LYP level) were added to the first VDE to obtain the second and higher VDEs. Core electrons were frozen when treating the electron correlation

† Part of the "Klaus Müller-Dethlefs Festschrift".

* Corresponding authors. E-mails: (K.H.B.) kbowen@jhu.edu, (A.I.B.) a.i.boldyrev@usu.edu.

10.1021/jp101419b
Published on Web 04/07/2010

at the RCCSD(T) and ROVGF levels of theory. The B3LYP, R(U)CCSD(T), R(U)OVGF, and TD-B3LYP calculations were performed using the Gaussian03 and Molpro programs.[43,44] Molecular structure visualization was done using the MOLDEN 3.4 program.[45]

IV. Experimental Results

The following cluster anion series were observed in the mass spectra: $Ga_xN_1^-$, $Ga_xN_2^-$, and Ga_x^-. We observed $Ga_xN_1^-$ species ranging from $x = 3$ to 12, with their intensity distributions reaching maxima between $x = 4$ and 7, depending on source conditions. In our source, it was difficult to make useable intensities for $Ga_xN_1^-$ species smaller than $Ga_4N_1^-$. Under favorable source conditions, $Ga_xN_2^-$ size distributions were also observed for $x = 7-12$. The observed Ga_x^- size distribution ranged from $x = 3$ to 17.

With the available ion intensities, we were able to measure photoelectron spectra of $Ga_xN_1^-$ cluster anions over the size range, $x = 4-12$ using both 3.49 and 4.66 eV photons. Their photoelectron spectra measured with 4.66 eV photons are presented in Figure 1. Their photoelectron spectra, measured with 3.49 eV photons, showed the same peaks and spectral features at the same electron binding energies up to the available photon energy, suggesting that anion resonances were not present in the photon energy range utilized. We were also able to record the photoelectron spectra of $Ga_xN_2^-$ over the size range, $x = 7-12$ using 3.49 eV photons, and they are presented in Figure 2. We furthermore measured the anion photoelectron spectra of Ga_x^- species having the same number of gallium atoms as the $Ga_xN_y^-$ cluster anions we studied, and they agreed with the spectra recorded earlier by Cha et al.[46]

The peaks in the photoelectron spectra correspond to photodetachment transitions from the ground vibronic state of a given $Ga_xN_y^-$ cluster anion to the ground and excited vibronic states of its neutral counterpart. The EBE values (listed as VDEs) of prominent peaks for the Ga_xN^- series and $Ga_7N_2^-$ cluster are presented in Tables 1−5. It is seen that the smaller members of the Ga_xN^- series exhibit rich electronic structure, indicating that their neutral cluster counterparts exhibit several low-lying electronic states. The spectrum of Ga_4N^- displays the greatest spacing between the first two peaks. In the spectra of both Ga_5N^- and Ga_6N^-, pairs of peaks are apparent. In the spectrum of Ga_5N^-, the spacing between peaks X and C is about the same as that between peaks A and D. In the spectrum of Ga_6N^-, the spacing between peaks X and B is about the same as that between peaks A and C. Furthermore, this spacing is smaller than the previously discussed spacing. The spectrum of Ga_7N^- stands apart from the others in that the EBE value of its lowest EBE peak is lower than all the other Ga_xN^- species, except for Ga_4N^-. Other than the case of Ga_7N, the EBE of the Ga_xN^- clusters all appear to be increasing with x.

The photoelectron spectra of the $Ga_xN_2^-$ cluster anions are less well-defined; that is, their peaks are broadened. Although their profiles are similar to both Ga_xN^- and Ga_x^- photoelectron spectra having the same number of gallium atoms, x, they lack some of the features of the Ga_x^- spectra. Moreover, it is quite unlikely that the cooling conditions of our source would have been cold enough to "solvate" Ga_x^- cluster anions with a N_2 molecule. It appears that the profiles of the $Ga_xN_2^-$ spectra mimic the Ga_xN^- spectra having the same x.

V. Theoretical Results

Ga_4N^-. We initially performed CK and GEGA searches for the global minimum of Ga_4N^- at the B3LYP/3-21G level of theory. Both methods revealed an identical global minimum structure I (D_{4h}, $^1A_{1g}$) (Figure 3). The geometries and frequencies for the low-lying structures of Ga_4N^- were then recalculated at the B3LYP/6-311+G* level of theory. Finally, single-point calculations for the three lowest-lying isomers were calculated at RCCSD(T)/6-311+G(2df) at the optimized B3LYP/6-311+G* geometries (except for structure I, for which the single-point calculations were performed at the optimized RCCSD(T)/6-311+G* geometry). Geometric structures, symmetries, electronic states, and relative energies of the first three low-lying isomers are displayed in Figure 3.

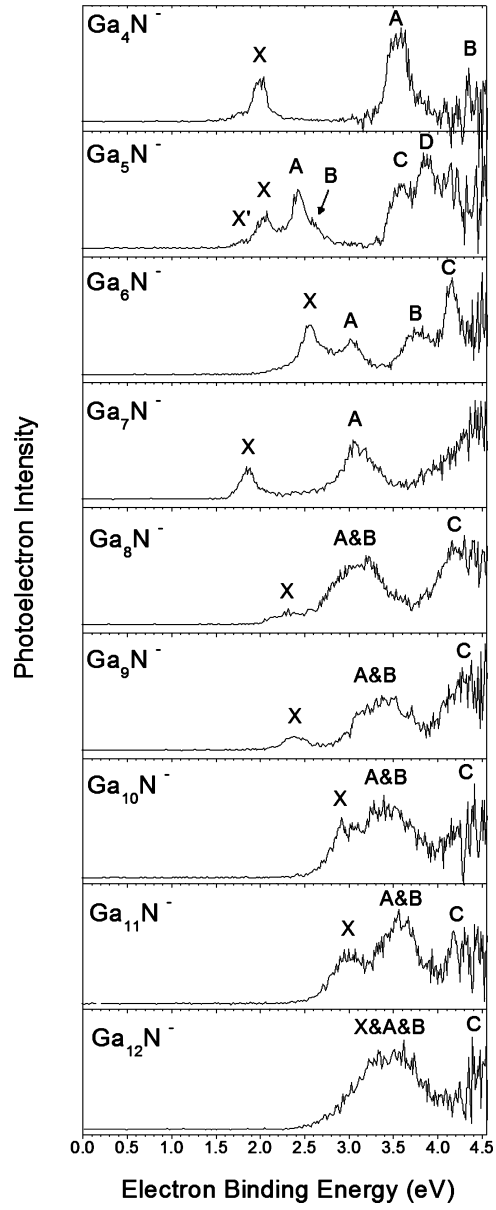

Figure 1. Photoelectron spectra of Ga_xN^-, $x = 4-12$, measured with 4.66 eV photons.

Both structures II and III are significantly higher in energy (by 18.9 and 20.3 kcal/mol at CCSD(T)/6-311+G(2df), respectively) and, thus, cannot contribute to the PES spectra. These two isomers will not be considered further. The same planar square global minimum structure of the congener Al_4N^- cluster was initially predicted computationally,[47–51] and then it was confirmed in a joint experimental and theoretical study by Averkiev et al.[52]

Ga_5N^-. The CK and GEGA global minimum searches revealed three structures, IV, V, and VI, of Ga_5N^- to be very

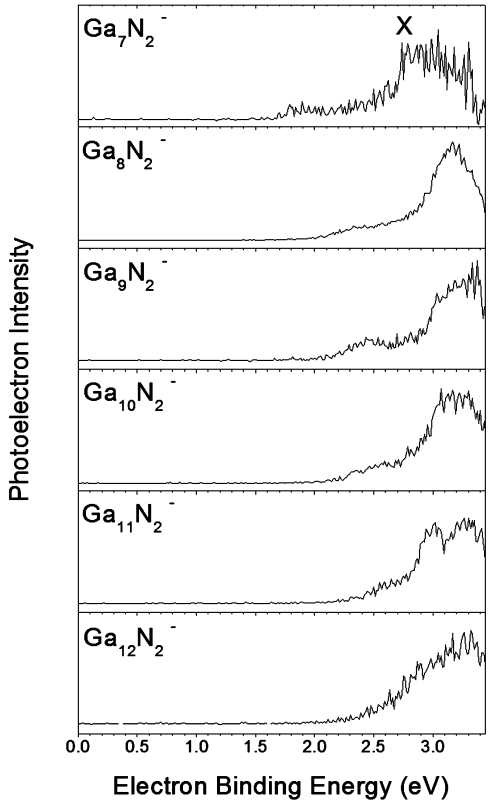

Figure 2. Photoelectron spectra of $Ga_xN_2^-$, $x = 7-12$, measured with 3.49 eV photons.

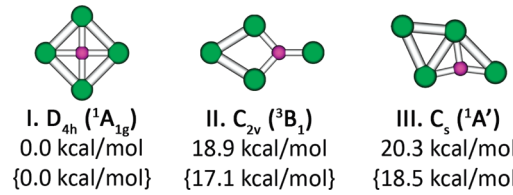

Figure 3. (a) The three lowest isomers of Ga_4N^-, their symmetries, spectroscopic states, and relative energies at CCSD(T)/6-311+G(2df) and at B3LYP/6-311+G* (in braces).

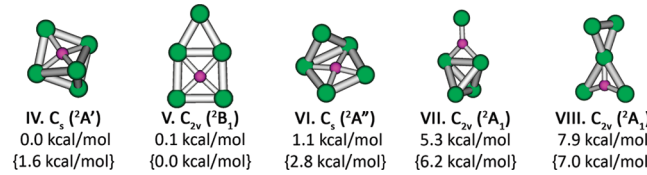

Figure 4. The five lowest isomers of Ga_5N^-, their symmetries, spectroscopic states, and relative energies at CCSD(T)/6-311+G(2df) and at B3LYP/6-311+G* (in braces).

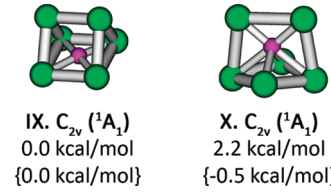

Figure 5. The two lowest isomers of Ga_6N^-, their symmetries, spectroscopic states, and relative energies at CCSD(T)/6-311+G(2df) and at B3LYP/6-311+G* (in braces).

close in energy (within 3 kcal/mol) at the B3LYP/3-21G level of theory (Figure 4). The geometries and frequencies for the first five low-lying structures of Ga_5N^- were then recalculated at the B3LYP/6-311+G* level of theory. Finally, single-point calculations for all the presented lowest-lying isomers were calculated at UCCSD(T)/6-311+G(2df) at the optimized B3LYP/6-311+G* geometries (Figure 4). The energies of the two lowest isomers IV and V are too close to one another (within 0.1 kcal/mol at CCSD(T)/6-311+G(2df)) to make a global minimum assignment on the basis of our calculations. Geometric structures, symmetries, electronic state, and relative energies of the first five low-lying isomers are displayed in Figure 4. The identified lowest isomers (IV, V, VI, VII, and VIII) are the same as for the congener cluster of Al_5N^-,[52] although the order of these isomers is different.

Ga_6N^-. Our CK and GEGA global minimum searches found the two lowest structures of Ga_6N^-, isomers IX and X, to be very close in energy (within 3 kcal/mol) at the B3LYP/3-21G level of theory (Figure 5). The geometries and frequencies for the first two low-lying structures of Ga_6N^- were then recalculated at the B3LYP/6-311+G* level of theory. Finally, single-point calculations for the two lowest isomers were calculated at RCCSD(T)/6-311+G(2df) at the optimized B3LYP/6-311+G* geometries (Figure 5). Geometric structures, symmetries, electronic states, and relative energies of isomers IX and X are displayed in Figure 5. The two lowest isomers of Ga_6N^- are the same as for the congener cluster of Al_6N^-.[53] Similarly to Al_6N^-, we found that other isomers of Ga_6N^- are significantly higher in energy and should not contribute to the experimental photoelectron spectra of the Ga_6N^- cluster.

Ga_7N^-. Our CK global minimum search found only one lowest structure of Ga_7N^-, isomer XI (Figure 6). However, when we recalculated alternative structures at the B3LYP/6-311+G* level of theory, we found that there were two low-lying isomers (XI and XII) (Figure 6). Finally, single-point calculations for the four lowest structures were calculated at RCCSD(T)/6-311+G(2df) at the optimized B3LYP/6-311+G* geometries (Figure 6). The relative energies of the four lowest structures calculated using the MOLPRO software package at the various coupled cluster methods, namely, RCCSD(T), RCCSD[T], RCCSD-T, UCCSD(T), UCCSD[T], UCCSD-T, are given in the Supporting Information (see Table S1). The results obtained using these methods differ by no more than 0.6 kcal/mol. The lowest isomer of Ga_7N^- is the same as for the congener cluster of Al_7N^-.[54] In the previous calculations of Al_7N^-, there were

TABLE 1: Experimentally Observed and Theoretically Calculated VDEs of Ga_4N^-[a]

feature	VDE (exptl), eV	final state and electronic configuration	VDE (theor), eV		
			TD-B3LYP[b]	OVGF[b,c]	ΔCCSD(T)[b]
X	2.0	$^2B_{2g}$, $1a_{2u}^2 1b_{1\,g}^2 2e_u^4 1b_{2g}^1$	1.93	1.99 (0.89)	2.01
A	3.6	^2E_u, $1a_{2u}^2 1b_{1g}^2 2e_u^3 1b_{2g}^2$	3.38	3.62 (0.86)	3.52
B	4.3	$^2B_{1g}$, $1a_{2u}^2 1b_{1g}^1 2e_u^4 1b_{2g}^2$	4.61	4.57 (0.82)	4.38

[a] Structure I D_{4h}, $^1A_{1g}$. All energies are in electronvolts. [b] Calculated using the 6-311+G(2df) basis set. [c] Values in parentheses represent the pole strength of the OVGF calculation.

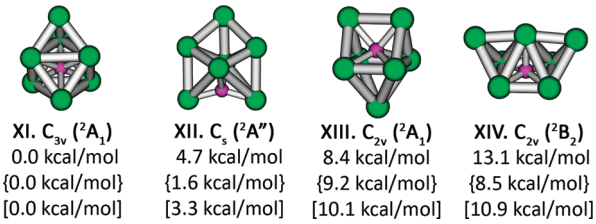

Figure 6. The lowest isomers of Ga_7N^-, their symmetries, spectroscopic states, and relative energies at CCSD(T)/6-311+G(2df), at B3LYP/6-311+G* (in braces), and at BPW91/6-311+G* (in square brackets).

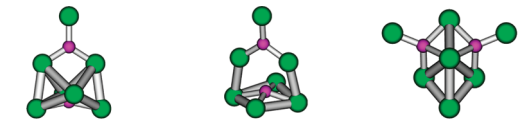

Figure 7. The lowest isomers of $Ga_7N_2^-$, their symmetries, spectroscopic states, and relative energies at CCSD(T)/6-311+G(2df) and at B3LYP/6-311+G* (in braces).

no other low-lying isomers. However, for Ga_7N^-, we found that the second-lowest isomer XII was 4.7 kcal/mol higher than the global minimum structure. The other two structures XIII and XIV were shown to have two imaginary frequency modes, as compared to that of the Al_7N^- cluster, in which they were both local minima lying higher in energy.[54] Following the geometry optimization along those frequencies leads to the global minimum structure (isomer XI). To test if these structures are, indeed, saddle points of the second order, we carried out geometry optimization and frequency calculations using a different nonhybrid density functional exchange correlation potential known in the literature as BPW91[55–58] using the same basis set (6-311+G*). At the BPW91/6-311+G* level, isomer XI is still a global minimum, and isomer XII is the second-lowest isomer, whereas structures XIII and XIV preserved the two imaginary modes, thus, leaving only two competitive isomers (XI and XII).

$Ga_7N_2^-$. According to our CK global minimum search, three lowest isomers of $Ga_7N_2^-$ (XV, XVI, and XVII) were identified (Figure 7). The two lowest isomers (XV and XVI) are degenerate at the B3LYP/6-311+G* level of theory, but the isomer XV is slightly more stable at RCCSD(T)/6-311+G(2df). Geometric and electronic properties of neutral Ga_nN_2 (n = 1−18) clusters have been investigated previously by Song and Cao at the DFT level (the generalized gradient approximation and full-potential linear-muffin-tin-orbital molecular dynamics method).[19] According to their calculations, starting from Ga_4N_2, the nitrogen molecule dissociates. For the neutral Ga_7N_2 cluster, they reported the global minimum structure, which becomes a saddle point upon addition of one electron. The geometry optimization of it following the imaginary frequency modes leads to the global minimum of $Ga_7N_2^-$, isomer XV. Isomer XVII is higher in energy by 2.7 kcal/mol than the global minimum (isomer XV) at RCCSD(T)/6-311+G(2df), but we still do not rule out the possibility of its contribution to the photoelectron spectrum.

The searches for the global minimum structures for clusters Ga_xN^-, where $x > 7$, and $Ga_xN_2^-$, x = 8−12, are too demanding, as for our computer resources. Therefore, we did not perform any theoretical calculations on those clusters.

VI. Interpretation of the PES Spectra

Ga_4N^-. The ab initio VDEs calculated at the TD-B3LYP/6-311+G(2df), ROVGF/6-311+G(2df) and R(U)CCSD(T)/6-311+G(2df) levels for the global minimum structure I of Ga_4N^- are compared with the experimental data in Table 1. The global minimum of Ga_4N^- was found to be the planar square structure I (D_{4h}, $^1A_{1g}$) with the valence electronic configuration $1a_{1g}^2 1e_u^4 2a_{1g}^2 1a_{2u}^2 1b_{1g}^2 2e_u^4 1b_{2g}^2$. As given in Table 1, our calculated VDE for the removal of an electron from the HOMO ($1b_{2g}$) of the global minimum is 2.01 eV at the ΔCCSD(T)/6-311+G(2df) level of theory (our highest level of theory), 1.99 eV at the ROVGF/6-311+G(2df) level of theory, and 1.93 eV at the TD-B3LYP/6-311+G(2df) level of theory. The pole strength (at the ROVGF level) of the 1 VDE was found to be 0.89, indicating that the detachment channel can be primarily described by a one-electron detachment process. This calculated first VDE for structure I is in excellent agreement with the measured VDE of 2.00 ± 0.10 eV for the X feature (Table 1 and Figure 1). The second and the third features (A and B) can be assigned to the removal of an electron from the HOMO-1 ($1b_{2g}$) and HOMO-2 ($2e_u$), respectively. Again, excellent agreement among all the levels of theory and the experiment was obtained for both VDEs (Table 1). Good agreement between experimental and theoretical VDEs for structure I is an unequivocal proof that this structure was, indeed, observed under the experimental conditions and that the planar square structure with a nitrogen atom at the center is, indeed, a global minimum structure of the Ga_4N^- cluster.

Ga_5N^-. According to our calculations, three isomers (IV, V, and VI) compete for the global minimum structure of Ga_5N^-. Structure IV (C_s, $^2A'$) has the valence electronic configuration $1a'^2 2a'^2 1a''^2 3a'^2 4a'^2 5a'^2 6a'^2 2a''^2 7a'^2 3a''^2 8a'^1$. The first VDE of the isomer IV corresponds to an electron detachment from the HOMO (8a′) resulting in the final lowest singlet state $^1A'$ with the electronic configuration: $1a'^2 2a'^2 1a''^2 3a'^2 4a'^2 5a'^2 6a'^2 2a''^2 7a'^2 3a''^2 8a'^0$. The second VDE of isomer IV corresponds to an electron detachment from the HOMO-1 (3a″), resulting in the final lowest triplet state $^3A''$ with the electronic configuration $1a'^2 2a'^2 1a''^2 3a'^2 4a'^2 5a'^2 6a'^2 2a''^2 7a'^2 3a''^1 8a'^1$. These first two VDEs calculated at our highest level of theory (ΔCCSD(T)/6-311+G(2df)) are in good agreement with the experimental values (features X and A) (see Table 2). The planar structure V (C_{2v}, $^2B_1$) has the valence electronic configuration, $1a_1^2 2a_1^2 1b_2^2 3a_1^2 4a_1^2 1b_2^2 2b_2^2 3b_2^2 5a_1^2 6a_1^2 2b_1^1$. The first VDE of isomer V corresponds to an electron detachment from the HOMO ($2b_1$), resulting in the final singlet state $^1A_1$ with the electronic configuration $1a_1^2 2a_1^2 1b_2^2 3a_1^2 4a_1^2 1b_2^2 2b_2^2 3b_2^2 5a_1^2 6a_1^2 2b_1^0$. Our calculated first VDE of isomer V is somewhat lower than the first VDE observed experimentally (feature X), but it may be responsible for the weak feature X′ occurring at about 1.8 eV, suggesting that isomer V is a minor contributor to the experimental PES. Theoretically calculated VDEs for isomer VI are very similar to those of structure IV, and thus, we cannot rule out the presence of isomer VI in a molecular beam.

Ga_6N^-. We identified two isomers IX (C_{2v} $^1A_1$, $1a_1^2 1b_1^2 1b_2^2 2a_1^2 3a_1^2 1a_2^2 2b_2^2 4a_1^2 2b_1^2 3b_2^2 5a_1^2 3b_1^2$) and X ($C_{2v}$ $^1A_1$, $1a_1^2 2a_1^2 1b_2^2 1b_1^2 3a_1^2 2b_2^2 4a_1^2 2b_1^2 5a_1^2 3b_2^2 1a_2^2 6a_1^2$), which could contribute to the experimental PES spectra of the Ga_6N^- cluster. Calculated VDEs for these two clusters are compared with the experimental VDEs in Table 3. One can see that the first four VDEs of isomer IX, corresponding to electron detachments from HOMO ($3b_1$), HOMO-1 ($5a_1$), HOMO-2 ($3b_2$), and HOMO-3 ($2b_1$), fit perfectly the experimental spectra, especially those VDEs calculated at the ΔCCSD(T)/6-311+G(2df) level of theory. For the second-lowest isomer of Ga_6N^- (isomer X), the

TABLE 2: Experimentally Observed and Theoretically Calculated VDEs of Ga_5N^-[a]

feature	VDE (exptl) eV	final state and electronic configuration	VDE (theor), eV TD-B3LYP[b]	UOVGF[b,c]	ΔCCSD(T)[b]
		Structure IV C_s, $^2A'$			
X	2.1	$^1A'$, $5a'^2 6a'^2 2a''^2 7a'^2 3a''^2 8a'^0$	1.94	2.27 (0.88)	2.01
A	2.4	$^3A''$, $5a'^2 6a'^2 2a''^2 7a'^2 3a''^1 8a'^1$	2.24	2.21 (0.88)	2.39
B	2.6	$^1A''$, $5a'^2 6a'^2 2a''^2 7a'^2 3a''^1 8a'^1$	2.42	*d*	*d*
C	3.6	$^3A'$, $5a'^2 6a'^2 2a''^2 7a'^1 3a''^2 8a'^1$	3.57	3.82 (0.86)	3.71
D	3.9	$^3A''$, $5a'^2 6a'^2 2a''^1 7a'^2 3a''^2 8a'^1$	3.85	*d*	*d*
		$^1A'$, $5a'^2 6a'^2 2a''^2 7a'^1 3a''^2 8a'^1$	3.88	4.01 (0.85)	*d*
		$^1A''$, $5a'^2 6a'^2 2a''^1 7a'^2 3a''^2 8a'^1$	3.96	*d*	*d*
		$^3A'$, $5a'^2 6a'^1 2a''^2 7a'^2 3a''^2 8a'^1$	4.06	4.24 (0.84)	*d*
		$^1A'$, $5a'^2 6a'^1 2a''^2 7a'^2 3a''^2 8a'^1$	4.36	*d*	*d*
		Structure V C_{2v}, $^2B_1$			
X′	~1.8	$^1A_1$, $1b_1^2 2b_2^2 3b_2^2 5a_1^2 6a_1^2 2b_1^0$	1.74	1.88 (0.88)	1.79
A	2.4	$^3B_1$, $1b_1^2 2b_2^2 3b_2^2 5a_1^2 6a_1^1 2b_1^1$	2.37	2.40 (0.87)	2.42
B	2.6	$^1B_1$, $1b_1^2 2b_2^2 3b_2^2 5a_1^2 6a_1^1 2b_1^1$	2.52	*d*	*d*
C	3.6	$^3B_1$, $1b_1^2 2b_2^2 3b_2^2 5a_1^1 6a_1^2 2b_1^1$	3.43	3.56 (0.83)	*d*
D	3.9	$^1B_1$, $1b_1^2 2b_2^2 3b_2^2 5a_1^1 6a_1^2 2b_1^1$	3.64	*d*	*d*
		$^3A_2$, $1b_1^2 2b_2^2 3b_2^1 5a_1^2 6a_1^2 2b_1^1$	3.84	4.10 (0.84)	4.01
		$^1A_2$, $1b_1^2 2b_2^2 3b_2^1 5a_1^2 6a_1^2 2b_1^1$	3.90	*d*	*d*
		Structure VI C_s, $^2A''$			
X	2.1	$^1A'$, $2a''^2 5a'^2 3a''^2 6a'^2 7a'^2 4a''^0$	1.96	2.12 (0.88)	2.03
A	2.4	$^3A''$, $2a''^2 5a'^2 3a''^2 6a'^2 7a'^1 4a''^1$	2.24	2.50 (0.88)	2.44
B	2.6	$^1A''$, $2a''^2 5a'^2 3a''^2 6a'^2 7a'^1 4a''^1$	2.50	*d*	*d*
C	3.6	$^3A''$, $2a''^2 5a'^2 3a''^2 6a'^1 7a'^2 4a''^1$	3.51	3.64 (0.85)	*d*
D	3.9	$^3A'$, $2a''^2 5a'^2 3a''^1 6a'^2 7a'^2 4a''^1$	3.66	3.92 (0.85)	3.86
		$^1A''$, $2a''^2 5a'^2 3a''^2 6a'^1 7a'^2 4a''^1$	3.69	*d*	*d*
		$^3A''$, $2a''^2 5a'^1 3a''^2 6a'^2 7a'^2 4a''^1$	4.42	4.62 (0.83)	*d*

[a] Structure IV C_s, $^2A'$; structure V C_{2v}, $^2B_1$; and structure VI C_s, $^2A''$. All energies are in electronvolts. [b] Calculated using the 6-311+G(2df) basis set. [c] Values in parentheses represent the pole strength of the OVGF calculation. [d] These values cannot be calculated at this level of theory.

TABLE 3: Experimentally Observed and Theoretically Calculated VDEs of Ga_6N^-[a]

feature	VDE (exptl)[b]	final State and electronic configuration	VDE (theor) TD-B3LYP[b]	OVGF[b,c]	ΔCCSD(T)[b]
		Structure IX C_{2v}, $^1A_1$			
X	2.5	$^2B_1$, $2b_2^2 4a_1^2 2b_1^2 3b_2^2 5a_1^2 3b_1^1$	2.36	2.43 (0.88)	2.51
A	3.0	$^2A_1$, $2b_2^2 4a_1^2 2b_1^2 3b_2^2 5a_1^1 3b_1^2$	2.91	3.00 (0.88)	3.05
B	3.8	$^2B_2$, $2b_2^2 4a_1^2 2b_1^2 3b_2^1 5a_1^2 3b_1^2$	3.58	3.68 (0.87)	3.63
C	4.1	$^2B_1$, $2b_2^2 4a_1^2 2b_1^1 3b_2^2 5a_1^2 3b_1^2$	3.99	4.31 (0.86)	*d*
		$^2A_1$, $2b_2^2 4a_1^1 2b_1^2 3b_2^2 5a_1^2 3b_1^2$	4.54	4.79 (0.82)	*d*
		Structure X C_{2v}, $^1A_1$			
X	2.5	$^2A_1$, $4a_1^2 2b_1^2 5a_1^2 3b_2^2 1a_2^2 6a_1^1$	2.45	2.61 (0.88)	2.67
A	3.0	$^2A_2$, $4a_1^2 2b_1^2 5a_1^2 3b_2^2 1a_2^1 6a_1^2$	2.57	2.77 (0.88)	2.79
B	3.8	$^2B_2$, $4a_1^2 2b_1^2 5a_1^2 3b_2^1 1a_2^2 6a_1^2$	3.97	4.28 (0.86)	4.17
C	4.1	$^2A_1$, $4a_1^2 2b_1^2 5a_1^1 3b_2^2 1a_2^2 6a_1^2$	4.00	4.04 (0.86)	*d*
		$^2B_1$, $4a_1^2 2b_1^1 5a_1^2 3b_2^2 1a_2^2 6a_1^2$	4.30	4.54 (0.82)	4.54
		$^2A_1$, $4a_1^1 2b_1^2 5a_1^2 3b_2^2 1a_2^2 6a_1^2$	4.57	4.52 (0.85)	*d*

[a] Structure IX C_{2v}, $^1A_1$; structure X C_{2v}, $^1A_1$. All energies are in electronvolts. [b] Calculated using the 6-311+G(2df) basis set. [c] Values in parentheses represent the pole strength of the OVGF calculation. [d] These values cannot be calculated at this level of theory.

calculated VDEs do not fit the experimental spectra. In particular, there is no theoretical VDE of the isomer X capable of explaining the B feature of the experimental spectrum at 3.76 eV. Thus, we concluded that isomer IX is certainly present in the experimental spectra, and it is a global minimum structure for the Ga_6N^- cluster. The second isomer X was found to be higher in energy than the global minimum by 2.2 kcal/mol at the CCSD(T)/6-311+G(2df) level of theory. Although we cannot completely rule out the presence of isomer X in the molecular beam, it should be a minor contributor to the experimental spectra.

Ga_7N^-. The global minimum structure of Ga_7N^- (isomer XI C_{3v}, $^2A_1$) has the valence electronic configuration $1a_1^2 2a_1^2 1e^4 3a_1^2 4a_1^2 2e^4 3e^4 5a_1^2 4e^4 6a_1^1$. The first VDE of isomer XI corresponds to an electron detachment from the HOMO ($6a_1^1$) resulting in the final lowest singlet state $^1A_1$ with the electronic configuration $1a_1^2 2a_1^2 1e^4 3a_1^2 4a_1^2 2e^4 3e^4 5a_1^2 4e^4 6a_1^0$. The second VDE of isomer XI corresponds to an electron detachment from the HOMO-1 (4e) resulting in the final lowest triplet state ^3E with the electronic configuration $1a_1^2 2a_1^2 1e^4 3a_1^2 4a_1^2 2e^4 3e^4 5a_1^2 4e^3 6a_1^1$. These first two VDEs of Ga_7N^- (isomer XI C_{3v}, $^2A_1$) (2.38 and 3.13 eV) calculated at our highest level of theory (ΔCCSD(T)/6-311+G(2df)) can be compared with the experimental values (1.9 and 3.1 eV corresponding to features X and A, respectively) in Table 4. The bigger variance of the first calculated VDE (at ΔCCSD(T)/6-311+G(2df)) from the experimentally obtained value is puzzling, especially if one were to take into account that values of NORM(A) in all the ΔCCSD(T)/6-311+G(2df)

TABLE 4: Experimentally Observed and Theoretically Calculated VDEs of Ga_7N^-[a]

feature	VDE (exptl) eV	final atate and electronic configuration	VDE (theor), eV TD-B3LYP[b]	UOVGF[b,c]	ΔCCSD(T)[b]
		Structure XI C_{3v}, $^2A_1$			
X	1.9	$^1A_1$, $4a_1^2 2e^4 3e^4 5a_1^2 4e^4 6a_1^0$	2.23	2.57 (0.88)	2.38
A	3.1	^3E, $4a_1^2 2e^4 3e^4 5a_1^2 4e^3 6a_1^1$	2.87	3.08 (0.87)	3.13
		^1E, $4a_1^2 2e^4 3e^4 5a_1^2 4e^3 6a_1^1$	3.09	*d*	*d*
		$^3A_1$, $4a_1^2 2e^4 3e^4 5a_1^1 4e^4 6a_1^1$	3.75	3.75 (0.87)	
		$^1A_1$, $4a_1^2 2e^4 3e^4 5a_1^1 4e^4 6a_1^1$	3.91	*d*	*d*
		^3E, $4a_1^2 2e^4 3e^3 5a_1^2 4e^4 6a_1^1$	4.28	4.49 (0.85)	*d*
		^1E, $4a_1^2 2e^4 3e^3 5a_1^2 4e^4 6a_1^1$	4.41	*d*	*d*
		Structure XII C_s, $^2A''$			
X	1.9	$^1A'$, $8a'^2 3a''^2 4a''^2 9a'^2 5a''^0$	2.31	*e*	2.39[f]
A	3.1	$^3A''$, $8a'^2 3a''^2 4a''^2 9a'^1 5a''^1$	2.49	*e*	2.70[f]
		$^1A''$, $8a'^2 3a''^2 4a''9a'^1 5a''^1$	2.67	*d*	*d*
		$^3A'$, $8a'^2 3a''^2 4a''^1 9a'^2 5a''^1$	2.78	*e*	2.98[f]
		$^1A'$, $8a'^2 3a''^2 4a''^1 9a'^2 5a''^1$	3.07	*d*	*d*
		$^3A'$, $8a'^2 3a''^1 4a''^2 9a'^2 5a''^1$	3.90	*e*	*d*
		$^3A''$, $8a'^1 3a''^2 4a''^2 9a'^2 5a''^1$	3.98	*e*	*d*
		$^1A'$, $8a'^2 3a''^1 4a''^2 9a'^2 5a''^1$	4.18	*d*	*d*

[a] Structure XI C_{3v}, $^2A_1$; structure XII C_s, $^2A''$. All energies are in electronvolts. [b] Calculated using the 6-311+G(2df) basis set. [c] Values in parentheses represent the pole strength of the OVGF calculation. [d] These values cannot be calculated at this level of theory. [e] These values are not reported due to the high spin contamination ($\langle S^2 \rangle = 1.47$). [f] The values are calculated at the RCCSD(T) level to avoid spin contamination.

TABLE 5: Experimentally Observed and Theoretically Calculated VDEs of $Ga_7N_2^-$[a]

feature	VDE (exptl)	final state and electronic configuration	VDE (theor) TD-B3LYP[b]	OVGF[b,c]	ΔCCSD(T)[b,e]
		Structure XV C_{2v}, $^1A_1$			
X	2.8	$^2A_2$, $7a_1^2 3b_1^2 3b_2^2 8a_1^2 4b_1^2 1a_2^1$	2.56	2.76 (0.88)	2.77
A		$^2B_1$, $7a_1^2 3b_1^2 3b_2^2 8a_1^2 4b_1^1 1a_2^2$	3.53	3.65 (0.86)	3.54
B		$^2A_1$, $7a_1^2 3b_1^2 3b_2^2 8a_1^1 4b_1^2 1a_2^2$	3.61	3.74 (0.86)	4.04
C		$^2B_2$, $7a_1^2 3b_1^2 3b_2^1 8a_1^2 4b_1^2 1a_2^2$	3.76	4.09 (0.87)	3.98
		Structure XVI C_{2v}, $^1A_1$			
X	2.8	$^2A_2$, $7a_1^2 3b_2^2 3b_1^2 4b_2^2 8a_1^2 1a_2^1$	2.55	2.75 (0.88)	2.73
A		$^2A_1$, $7a_1^2 3b_2^2 3b_1^2 4b_2^2 8a_1^1 1a_2^2$	3.52	3.67 (0.86)	3.74
B		$^2B_2$, $7a_1^2 3b_2^2 3b_1^2 4b_2^1 8a_1^2 1a_2^2$	3.70	3.81 (0.85)	3.71
C		$^2B_1$, $7a_1^2 3b_2^2 3b_1^1 4b_2^2 8a_1^2 1a_2^2$	3.78	4.15 (0.86)	4.00
		Structure XVII C_s, $^1A'$			
X	2.8	$^2A'$, $7a'^2 5a''^2 8a'^2 6a''^2 9a'^2 10a'^1$	2.29	2.50 (0.88)	2.51
A		$^2A'$, $7a'^2 5a''^2 8a'^2 6a''^2 9a'^1 10a'^2$	3.11	3.41 (0.87)	*d*
B		$^2A''$, $7a'^2 5a''^2 8a'^2 6a''^1 9a'^2 10a'^2$	3.67	4.20 (0.85)	
C		$^2A'$, $7a'^2 5a''^2 8a'^1 6a''^2 9a'^2 10a'^2$	3.73	4.23 (0.86)	*d*

[a] Structure XV C_{2v}, $^1A_1$; structure XVI C_{2v}, $^1A_1$; and structure XVII C_s, $^1A'$. All energies are in electronvolts. [b] Calculated using the 6-311+G(2df) basis set. [c] Values in parentheses represent the pole strength of the OVGF calculation. [d] These values cannot be calculated at this level of theory. [e] At RCCSD(T) method.

calculations are within the range where single configuration approximation is reasonable (1.28 for the anion in $^2A_1$ state, and 1.25 for the corresponding neutral $^1A_1$ state). To further address this issue, we performed additional CASSCF-MRCISD calculations with a different choice of active space in the CASSCF expansion (number of active electrons, number of active orbitals): (5, 4), (5, 6), (7, 8) for the doublet anion and (4, 4), (4, 6), (6, 8) for the corresponding neutral singlet species. These calculations were performed using the 6-311+G* basis set. The first calculated VDE was found to be 1.85, 1.87, 1.84 eV when the following active spaces are used: ((5, 4) anion/(4, 4) neutral), ((5, 6) anion/(4, 6) neutral), and ((7, 8) anion/(6, 8) neutral), respectively. These results are in excellent agreement with the experimentally obtained 1VDE; thus, the multiconfigurational nature of the wave function could be responsible for the deviation of the ΔCCSD(T)/6-311+G(2df) results from the experiment. However, taking into account a rather moderate basis set and limited active space, these results should be considered as preliminary ones.

The results of the experimentally observed and theoretically calculated VDEs of the second lowest isomer XII of Ga_7N^- (C_s, $^2A''$) are also presented in Table 4. Both of the first two VDEs calculated for this isomer significantly differ from the experimentally obtained values (Table 4). Thus, we can rule out the presence of relatively high-lying isomer XII in a molecular beam leaving only one isomer of Ga_7N^- (isomer XI C_{3v}, $^2A_1$) as the major contributor to the experimental photoelectron spectrum.

$Ga_7N_2^-$. The VDEs for all three lowest isomers of the $Ga_7N_2^-$ cluster (see Figure 7) are presented in Table 5. The first VDEs calculated for isomers XV and XVI (2.77 and 2.73 eV, respectively) at our highest level of theory are nearly the same and are in good agreement with the experimentally observed feature X of 2.8 eV. The first VDE calculated for isomer XVII, which lies higher in energy by 2.7 kcal/mol, is somewhat lower (2.51 eV) than the value corresponding to the feature X (2.8 eV) and could be responsible for the weak, not well-resolved feature prior to feature X in the experimental PES. We cannot

rule out the presence of isomer XVII in a molecular beam, but if it is present, then it is present only as a minor contributor.

VII. Discussion

In this article, we have reported anion photoelectron spectra of $Ga_xN_y^-$ cluster anions, where $x = 4-12$, $y = 1$ and $x = 7-12$, $y = 2$. In the follow-up ab initio calculations, we perfomed the global minimum search for $Ga_xN_y^-$ cluster anions, where $x = 4-7$, $y = 1$, and $Ga_7N_2^-$ using two theoretical methods: the Gradient Embedded Genetic Algorithm and the Coalescence Kick methods. Theoretical VDEs for the global minimum structures and low-lying isomers were compared to the experimental VDEs, thus allowing the identification of the isomers present in the beam experiments of specific Ga_xN^- cluster anions ($x = 4-7$) and the $Ga_7N_2^-$ cluster.

In the current study, we have showed that the global minimum structures found for Ga_xN^- clusters ($x = 4-7$) are mostly the same as those of previously reported global minimum structures of their congener Al_xN^- clusters ($x = 4-7$).[52–54] However, in a few cases, we found that the sets of low-lying isomers for Ga_xN^- clusters ($x = 4-7$) can differ from those in Al_xN^- clusters ($x = 4-7$).

The case of the observed series of $Ga_xN_2^-$ cluster anions is curious. Gallium nitride cluster anions with more than one nitrogen atom were not observed in the previous study.[5] One might well imagine that their absence was due to the strength of the nitrogen−nitrogen bond and that any attempts to add additional nitrogen atoms would simply result in the formation of N_2 and its escape. Nevertheless, they exist. We observe them in our mass spectra, and we have recorded their photoelectron spectra. The similarity of their photoelectron spectra to those of Ga_xN^- would seem to suggest that the second nitrogen atom acts as a disinterested spectator or "solvent", but this seems chemically absurd given the strength of the nitrogen−nitrogen bond. According to our calculations, the nitrogen−nitrogen bond is broken in the $Ga_7N_2^-$ cluster, in agreement with the previously reported theoretical study by Song and Cao,[19] who predicted that starting from Ga_4N_2, the nitrogen molecule dissociates. Reasonable agreement between theoretical and experimental results for VDEs of $Ga_7N_2^-$ provides additional proof for the presence of a $Ga_7N_2^-$ cluster with dissociated nitrogen molecule. This result provides the first clue that the nitrogen molecule should also be present in the experimentally observed larger $Ga_xN_2^-$ clusters ($x = 7-12$) as two separated nitrogen atoms embedded in gallium clusters. Dinitrogen gallium clusters could be a good platform for understanding how the second-strongest (after C≡O) chemical bond in diatomic molecules can be broken upon interaction with atomic clusters.

Acknowledgment. The theoretical work done at Utah State University was supported by the National Science Foundation (CHE-0714851). Computer time from the Center for High Performance Computing at Utah State University is gratefully acknowledged. The computational resource, the Uinta cluster supercomputer, was provided through the National Science Foundation under Grant CTS-0321170 with matching funds provided by Utah State University. The experimental work was done at Johns Hopkins University and was supported by a grant from the Air Force Office of Scientific Research.

Supporting Information Available: The relative energies of the four lowest structures of Ga_7N^- calculated using MOLPRO software package at the various CCSDT methods are given in the Supporting Information in Table S1. This material is available free of charge via the Internet at http://pubs.acs.org.

References and Notes

(1) *GaN and Related Materials*; Pearton, S. J., Ed.; Gordon and Breach: New York, 1997.
(2) Waltereit, P.; Brandt, O.; Trampert, A.; Grahn, H. T.; Menninger, J.; Ramsteiner, M.; Reiche, M.; Ploog, K. H. *Nature* **2000**, *406*, 865.
(3) Zhou, M.; Andrews, L. *J. Phys. Chem. A* **2000**, *104*, 1648.
(4) Himmel, H. J.; Hebben, N. *Chem.—Eur. J.* **2005**, *11*, 4096.
(5) Sheehan, S. M.; Meloni, G.; Parsons, B. F.; Wehres, N.; Neumark, D. M. *J. Chem. Phys.* **2006**, *124*, 064303.
(6) Kandalam, A. K.; Pandey, R.; Blanco, M. A.; Costales, A.; Recio, J. M.; Newsam, J. M. *J. Phys. Chem. B* **2000**, *104*, 4361.
(7) Kandalam, A. K.; Blanco, M. A.; Pandey, R. *J. Phys. Chem. B* **2001**, *105*, 6080.
(8) Kandalam, A. K.; Blanco, M. A.; Pandey, R. *J. Phys. Chem. B* **2002**, *106*, 1945.
(9) BelBruno, J. J. *Heteroat. Chem.* **2000**, *11*, 281.
(10) Costales, A.; Pandey, R. *J. Phys. Chem. A* **2003**, *107*, 191.
(11) Song, B.; Cao, P. L. *Phys. Lett. A* **2002**, *300*, 485.
(12) Song, B.; Cao, P. L. *Chin. Phys. Lett.* **2003**, *20*, 1488.
(13) Song, B.; Cao, P. L. *Phys. Lett. A* **2002**, *306*, 57.
(14) Song, B.; Cao, P. L.; Li, B. X. *Phys. Lett. A* **2003**, *315*, 308.
(15) Zhao, J.; Wang, B. L.; Zhou, X. L.; Chen, X. Sh.; Lu, W. *Chem. Phys. Lett.* **2006**, *422*, 170.
(16) Costales, A.; Kandalam, A. K.; Pendas, A. M.; Blanco, M. A.; Recio, J. M.; Pandey, R. *J. Phys. Chem. B* **2000**, *104*, 4368.
(17) Wang, Ch. Sh.; Balasubramanian, K. *Chem. Phys. Lett.* **2005**, *402*, 294.
(18) Song, B.; Cao, P. L. *Phys. Lett. A* **2004**, *328*, 364.
(19) Song, B.; Cao, P. L. *Phys. Lett. A* **2007**, *366*, 324.
(20) Costales, A.; Blanco, M. A.; Pendas, A. M.; Kandalam, A. K.; Pandey, R. *J. Am. Chem. Soc.* **2002**, *124*, 4116.
(21) Tafipolsky, M.; Schmid, R. *Chem. Vap. Deposition* **2007**, *13*, 84.
(22) Yadav, P. S.; Yadav, R. K.; Agrawal, B. K. *J. Phys.: Condens. Matter* **2007**, *19*, 079209.
(23) Gerhards, M.; Zheng, W.-J.; Thomas, O. C.; Lippa, T.; Xu, S.-J.; Bowen, K. H. *J. Chem. Phys.* **2002**, *124*, 144304.
(24) Alexandrova, A. N.; Boldyrev, A. I.; Fu, Y.-J.; Wang, X. B.; Wang, L. S. *J. Chem. Phys.* **2004**, *121*, 5709.
(25) Alexandrova, A. N.; Boldyrev, A. I. *J. Chem. Theory Comput.* **2005**, *1*, 566.
(26) Averkiev, B. B. *Geometry and Electronic Structure of Doped Clusters via The Coalescence Kick Method*; Ph.D. Dissertation, Utah State University: Logan, UT, 2009.
(27) Becke, A. D. *J. Chem. Phys.* **1993**, *98*, 5648.
(28) Vosko, S. H.; Wilk, L.; Nusair, M. *Can. J. Phys.* **1980**, *58*, 1200.
(29) Lee, C.; Yang, W.; Parr, R. G. *Phys. Rev. B* **1988**, *37*, 785.
(30) Cizek, J. *Adv. Chem. Phys.* **1969**, *14*, 35.
(31) Knowles, P. J.; Hampel, C.; Werner, H.-J. *J. Chem. Phys.* **1993**, *99*, 5219.
(32) Raghavachari, K.; Trucks, G. W.; Pople, J. A.; Head-Gordon, M. *Chem. Phys. Lett.* **1989**, *157*, 479.
(33) Binkley, J. S.; Pople, J. A.; Hehre, W. J. *J. Am. Chem. Soc.* **1980**, *102*, 939. Gordon, M. S.; Binkley, J. S.; Pople, J. A.; Pietro, W. J.; Hehre, W. J. *J. Am. Chem. Soc.* **1982**, *104*, 2797. Pietro, W. J.; Francl, M. M.; Hehre, W. J.; Defrees, D. J.; Pople, J. A.; Binkley, J. S. *J. Am. Chem. Soc.* **1982**, *104*, 5039.
(34) McLean, A. D.; Chandler, G. S. *J. Chem. Phys.* **1980**, *72*, 5639.
(35) Clark, T.; Chandrasekhar, J.; Spitznagel, G. W.; Schleyer, P. v. R. *J. Comput. Chem.* **1983**, *4*, 294.
(36) Cederbaum, L. S. *J. Phys. B* **1975**, *8*, 290.
(37) Ortiz, J. V. *Int. J. Quantum Chem., Quantum Chem. Symp.* **1989**, *23*, 321. Lin, J. S.; Ortiz, J. V. *Chem. Phys. Lett.* **1990**, *171*, 197.
(38) Zakrzewski, V. G.; Ortiz, J. V.; Nichols, J. A.; Heryadi, D.; Yeager, D. L.; Golab, J. T. *Int. J. Quantum Chem.* **1996**, *60*, 29.
(39) Dahnovsky, Y. *J. Chem. Phys.* **2007**, *126*, 234111.
(40) Kletsov, A.; Dahnovsky, Y. *Phys. Rev. B* **2007**, *76*, 035304.
(41) Bauernshmitt, R.; Alrichs, R. *Chem. Phys. Lett.* **1996**, *256*, 454.
(42) Casida, M. E.; Jamorski, C.; Casida, K. C.; Salahub, D. R. *J. Chem. Phys.* **1998**, *108*, 4439.
(43) Frisch, M. J.; Trucks, G. W.; Schlegel, H. B.; et al. *Gaussian03, revision D.01*; Gaussian, Inc.: Wallingford, CT, 2004.
(44) Werner, H.-J.; Knowles, P. J.; Lindh, R.; Manby, F. R.; Schütz, M.; et al. *MOLPRO*, version 2006.1: a package of ab initio programs; see http://www.molpro.net.
(45) Schaftenaar, G. *MOLDEN3.4*; CAOS/CAMM Center: The Netherlands, 1998.

(46) Cha, C.-Y.; Gantefoer, G.; Eberhardt, W. *J. Chem. Phys.* **1994**, *100*, 995.

(47) Schleyer, P. v. R.; Boldyrev, A. I. *J. Chem. Soc. Chem. Comm.* **1991**, 1536.

(48) Zakrzewski, V. G.; Niessen, W. v.; Boldyrev, A. I.; Schleyer, P. v. R. *Chem. Phys.* **1993**, *174*, 167.

(49) Nayak, S. K.; Rao, B. K.; Jena, P.; Li, X.; Wang, L. S. *Chem. Lett.* **1999**, *301*, 379.

(50) Boo, B. H.; Liu, Z. *J. Phys. Chem. A* **1999**, *103*, 1250.

(51) Leskiw, B. R.; Castleman, A. W., Jr.; Ashman, C.; Khanna, S. N. *J. Chem. Phys.* **2001**, *114*, 1165.

(52) Averkiev, B. B.; Boldyrev, A. I.; Li, X.; Wang, L. S. *J. Chem. Phys.* **2006**, *125*, 124305.

(53) Averkiev, B. B.; Boldyrev, A. I.; Li, X.; Wang, L. S. *J. Phys. Chem. A* **2007**, *111*, 34.

(54) Averkiev, B. B.; Call, S.; Boldyrev, A. I.; Wang, L. M.; Huang, W.; Wang, L. S. *J. Phys. Chem. A* **2008**, *112*, 1873.

(55) Becke, A. D. *Phys. Rev. A* **1988**, *38*, 3098.

(56) Perdew, J. P.; Chevary, J. A.; Vosko, S. H.; Jackson, K. A.; Pederson, M. R.; Singh, D. J.; Fiolhais, C. *Phys. Rev. B* **1992**, *46,* 6671.

(57) Perdew, J. P.; Chevary, J. A.; Vosko, S. H.; Jackson, K. A.; Pederson, M. R.; Singh, D. J.; Fiolhais, C. *Phys. Rev. B* **1993**, *48,* 4978.

(58) Perdew, J. P.; Burke, K.; Wang, Y. *Phys. Rev. B* **1996**, *54*, 16533.

JP101419B